

Optimization Methodology for Designing 2-CPAs Exploiting Pattern Diversity in Clustered MIMO Channels

Antonio Forenza, *Member, IEEE*, and Robert W. Heath, Jr., *Senior Member, IEEE*

Abstract—Arrays designed for multiple-input multiple-output (MIMO) communication systems must provide good performance in terms of information theoretic and microwave theoretic performance measures for a large number of channel scenarios. Consequently, the general MIMO array design problem is challenging. This paper proposes a novel optimization methodology for designing circular patch arrays (CPAs), under a clustered MIMO channel model assumption. Based on the ergodic capacity, it is found that the single-cluster scenario can approximate CPA performance in clustered channels, reducing the number of channel scenarios that need to be considered. Using a new definition of channel spatial correlation that allows for pattern diversity, metrics are derived for evaluating average and outage capacity performance of CPAs, which can be expressed as a function of only the antenna parameters. With this expression, an optimization is formulated and solved numerically for optimizing the parameters of a 2-CPA on a capacity based objective function and microwave theory performance constraints. An example design is given corresponding to a 2-CPA in the 2.4 GHz unlicensed frequency band.

Index Terms—MIMO systems, antenna arrays, pattern diversity, microstrip antennas, spatially correlated channels.

I. INTRODUCTION

THE capacity that a multiple-input multiple-output (MIMO) channel can support is a function of the array parameters (i.e., element spacing, array geometry, radiation pattern, cross-polarization) and the spatial characteristics of the propagation environment (i.e., angle spread, angle of arrival, power angle profile) [1]–[3]. MIMO antenna arrays can be designed to reduce the spatial correlation of the channel, resulting in enhanced link performance. One promising solution to reduce the spatial correlation is pattern diversity [4]–[11].

Pattern diversity can provide similar performance gains as conventional space diversity techniques [1]–[3], [12], [13], while satisfying more restrictive size constraints of wireless devices. To exploit pattern diversity, each antenna element is designed to radiate with near-orthogonal radiation patterns as

a means to create uncorrelated channels across different array elements. The benefits of pattern diversity have been shown through practical measurements with array designs employing tri-monopole collocated antennas [7], [8], switched parasitic antennas [4], [10], [14] and dipoles with 90° hybrid [5]. In [11] we derived the theoretical performance gain attainable through pattern over space diversity, by employing 2-element arrays of circular patch antennas, called circular patch arrays (CPAs).

Motivated by the theoretical results in [11], in this paper we define a novel optimization algorithm for designing 2-CPAs, accounting for both far-field (i.e., scattering in the propagation environment) and near-field (i.e., mutual coupling) effects. Complete models to analyze the performance of compact MIMO arrays were proposed in [15], [16]. In [15], [16] the transfer function of MIMO systems (relating the input signals to the output of the receiver) was defined to model the propagation channel as well as the coupled transmit and receive antennas. These models can be used to evaluate the performance of given MIMO array designs in different propagation scenarios via Monte Carlo simulations. To optimize the array parameters in a variety of propagation conditions, however, it is desirable to express the array performance (i.e., objective function of the optimization problem) as a deterministic function, thereby increasing the rate of convergence of the optimization algorithm. In this paper we decouple near-field and far-field effects, and define an objective function from closed form MIMO capacity expressions that account for the propagation channel.

Different solutions have been proposed in the literature for antenna design optimization [17]–[23]. These methods were conceived to optimize antenna bandwidth [17]–[21] and radiation pattern [22], [23], without accounting for far-field effects in the propagation channel. In MIMO communication, however, the capacity and error rate performance of antenna arrays are affected by the spatial correlation [24], which is in fact a function of the distribution of the scatterers in the propagation environment [1], [3]. Hence, optimization methods for MIMO array designs have to account for both far- and near-field effects. In this paper we propose a practical optimization algorithm to design MIMO arrays that exploit pattern diversity (i.e., CPAs) in realistic clustered propagation environments. We define the objective function for the optimization method based on MIMO communication performance metrics (to account for the propagation channel) and use microwave theory

Paper approved by A. Lozano, the Editor for Network Access and Performance of the IEEE Communications Society. Manuscript received October 31, 2006; revised March 31, 2007. This work is supported in part by the National Science Foundation under grant CCF-514194 and the Office of Naval Research under grant number N00014-05-1-0169.

A. Forenza is with Rearden, LLC, San Francisco, CA 94107 USA (e-mail: antonio@rearden.com).

R. W. Heath is with the Department of Electrical and Computer Engineering, The University of Texas at Austin, Austin, TX 78712-0240 USA (e-mail: rhealth@ece.utexas.edu).

Digital Object Identifier 10.1109/TCOMM.2008.060582

performance constraints (to ensure acceptable return loss and low mutual coupling).

To develop the proposed optimization methodology, first we discuss the channel and antenna parameters used as inputs to the optimization algorithm for CPA designs. We observe that the CPA performance in clustered channel models depends on orientation and angle spread of the clusters in the propagation environment. Since the CPA can not easily be reconfigured in practice, an alternative is to design a CPA that is robust to a suite of channel conditions. Unfortunately, this requires evaluating many different cluster configurations including cluster location and angle spread. To solve this problem, we demonstrate that the CPA performance can be measured in single-cluster channels over a reduced set of channel parameters with minimal error. This result makes the proposed array optimization algorithm in clustered MIMO channel models feasible since only a single cluster needs to be considered. Since the CPA uses pattern diversity not spatial diversity, we propose a new definition of spatial correlation more suitable for studies of pattern diversity in realistic clustered channel models. From this definition, we derive the MIMO ergodic capacity in correlated channels and define two communication theoretic metrics, which measure average and outage performance of CPAs in several different propagation scenarios. We express these metrics only as a function of the antenna parameters to be directly used in the optimization algorithm.

We account for near-field effects around the CPAs by defining the antenna bandwidth from the scattering parameters [25]. Theoretical analyses of the impedance bandwidth of circular microstrip antennas as a function of the physical antenna parameters were presented in [26], [27]. Here, we exploit the results in [26], [27] to evaluate bandwidth and mutual coupling effects as a function of the antenna parameters (i.e., radius of the circular patch, feed position). Based on these results, we propose a novel optimization algorithm that maximizes an objective function that considers both average and outage capacity, and uses microwave theory performance metrics to produce robust CPA designs. To make our discussion concrete, we consider practical system parameters (i.e., the ISM band) and clustered channel models as in the IEEE 802.11n standard for wireless local area networks (WLANs). While the proposed optimization methodology is conceived for 2-CPAs, we believe it can be extended (with appropriate choice of optimization parameters and design constraints) to any MIMO array that exploits pattern diversity in realistic clustered propagation environments.

This paper differs in several ways from our prior work in [11], [28]. In our prior work we derived the spatial correlation matrix for the 2-CPA under a single cluster assumption, found its eigenvalues, and then determined bounds on capacity and error rate. Using these results, we showed that performance gains due to pattern diversity are essentially determined by the shape of the antenna radiation patterns. In our previous work we analyzed the 2-CPA using ideal radiation patterns derived from theoretical analysis, while in this paper we evaluate these patterns numerically through an electromagnetic (EM) software tool, to account for the near-field effects. In our previous work, we only optimized the mode number of

the CPA using an argument about diminishing returns in the capacity for a specific choice of radius and feed location. In this paper we optimize the parameters of the 2-CPA based on a robustness objective function defined from average and outage ergodic capacities and we include constraints on the return loss and mutual coupling.

This paper is organized as follows. Section II describes the channel model and antenna parameters used in the proposed optimization method. Section III presents the CPA analysis in clustered MIMO channels. Sections IV and V describe the MIMO communication and microwave theory performance metrics for the optimization method, respectively. In Section VI we formulate and solve the proposed optimization algorithm. Finally, we draw the conclusions in Section VII.

II. OPTIMIZATION PARAMETERS AND PROBLEM FORMULATION

In this section we present the channel model and antenna parameters used in the proposed optimization algorithm for CPAs. Then we describe the optimization problem and algorithm block diagram.

A. Clustered MIMO Channel Model and Parameters

We generate the MIMO channel through the well known Kronecker model [1], [29]. While we recognize the fundamental limitations of this model [30]–[33], we adopt the Kronecker structure for its practical use in the IEEE 802.11n standard [34] and simple analytical tractability, which enables performance predictions of MIMO arrays with reduced computational complexity. For a narrowband MIMO system, with N_t transmit antennas and N_r receive antennas, the channel matrix under the Kronecker assumption is given by

$$\mathbf{H} = \mathbf{R}^{1/2} \mathbf{Z} \mathbf{S}^{1/2} \quad (1)$$

where $\mathbf{Z} \in \mathbb{C}^{N_r \times N_t}$ is a matrix of complex Gaussian fading coefficients. \mathbf{S} and \mathbf{R} denote the transmit and receive spatial correlation matrices.

In clustered channel models, the scattering objects around the transmit/receive arrays are modelled as “clusters” and are used to generate \mathbf{S} and \mathbf{R} . Detailed description of clustered MIMO channel models was provided in [11]. Here, we assume the clusters are distributed only over the azimuth directions, consistent to the measurement results in [35], and summarize the *channel parameters* as follows:

- **Number of clusters** (N_c);
- **Mean AOA** of the clusters: $\Phi = [\phi_c^{(1)}, \dots, \phi_c^{(N_c)}]$, with $\phi_c^{(i)} \in \mathcal{A}_\phi$;
- **Angle spread** of the clusters: $\Sigma = [\sigma_\phi^{(1)}, \dots, \sigma_\phi^{(N_c)}]$, with $\sigma_\phi^{(i)} \in \mathcal{A}_\sigma$;

where \mathcal{A}_ϕ and \mathcal{A}_σ denote the set of values of $\phi_c^{(i)}$ and $\sigma_\phi^{(i)}$, respectively. For example, the IEEE 802.11n channel model [34] assumes $\mathcal{A}_\phi = [0^\circ, 360^\circ]$ and $\mathcal{A}_\sigma = [15^\circ, 50^\circ]$.

B. Circular Patch Array (CPA) Model and Parameters

We study the performance of MIMO arrays consisting of two stacked circular microstrip antennas. The properties of

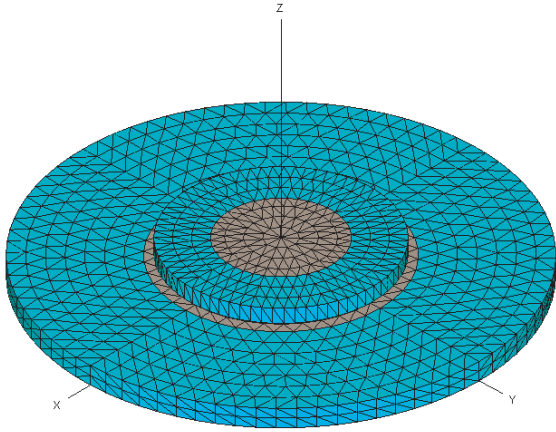


Fig. 1. Geometry of the 2-CPA design.

circular microstrip antennas have been studied in [26], [27], [36], [37]. In [27] it was shown that circular patch antennas operating with different modes produce different radiation patterns in far-field. In [11], [28] we exploited the orthogonality of the radiation patterns of circular patch antennas as a means to reduce the correlation between the elements of MIMO arrays, resulting in improved system performance (due to pattern diversity). We also showed the dependence of the array performance on mode number and physical antenna size, and found that mode number 3 provides good size/performance tradeoff.

In this paper, we consider 2-element CPAs with collocated antennas stacked on top of each other, as depicted in Fig. 1. We excite the two circular microstrip antennas via coaxial feeds, with $\phi_0 = \pi/(2n)$ angle difference to produce near-orthogonal radiation patterns as in [11]. The two microstrip antennas may have different physical dimensions, but the same mode number.

In summary, the physical *antenna parameters* describing the two elements of CPAs are:

- **Physical radius** (ρ_o) of the circular microstrip antennas;
- **Feed radial position** (ρ_f): defined as the distance between the center of the circular patch antenna and the feeding point (assuming coaxial feed);
- **Height** (h) of the antenna substrate;
- **Dielectric constant** (ϵ_r) of the antenna substrate;

where ρ_f is defined in the range $[0, \rho_o]$ and typically $\epsilon_r \in [2.2, 12]$.

C. Problem Statement

The goal of the algorithm proposed in this paper is to numerically compute the antenna parameters to optimize the CPA performance (according to metrics defined later in this paper) in a variety of propagation scenarios, determined by different combinations of channel parameters.

The optimization parameters are defined by the following vector describing the physical dimension of the m -th antenna element of the CPA

$$\mathbf{x}_m = \left[\rho_o^{(m)}, \rho_f^{(m)}, h^{(m)} \right] \quad (2)$$

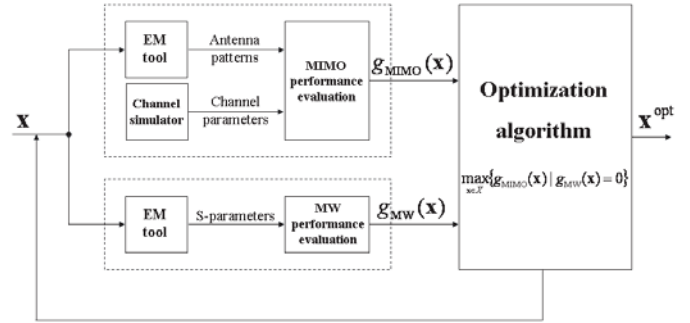


Fig. 2. Block diagram of the proposed optimization algorithm for MIMO array designs exploiting pattern diversity.

where $m \in \{1, 2\}$ for 2-element arrays¹ and $\mathbf{x} = [\mathbf{x}_1, \mathbf{x}_2]$ contains the physical parameters of the 2-CPA. The vector \mathbf{x} takes its values from the set $\mathcal{X} \subset \mathbb{R}^6$ that defines the physical constraints of the array design and the *feasible set* for the optimization algorithm. Note that \mathbf{x} may also contain additional entries, such as the dielectric constant (ϵ_r), the radius of the circular ground plane (ρ_{gp}) and the coaxial feed pin (r_c).

Fig. 2 shows the block diagram of the proposed optimization algorithm for MIMO array designs. For given input \mathbf{x} , the antenna patterns are computed numerically through EM software tools and used in combination with the channel parameters to predict the performance of MIMO arrays in correlated channels. Different communication theoretic metrics can be used to evaluate the performance of the array (i.e., capacity or error rate). In this paper we use the MIMO ergodic capacity [38]. As depicted in Fig. 2, from the EM tools we also compute the scattering parameters (i.e., the S-matrix) to measure the antenna bandwidth and mutual coupling effects. These performance metrics are fed to the optimization algorithm that computes the optimal set of antenna parameters \mathbf{x}^{opt} .

We observe that optimal CPA designs obtained from this method have to be robust in a variety of propagation conditions. It is impractical, however, to evaluate the CPA performance for any combination of orientation and angle spread of the clusters, defined by the channel parameters in Subsection II-A. In the next section, we demonstrate how to choose a subset of channel parameters for the proposed optimization algorithm based on capacity analysis.

III. CPA ANALYSIS IN CLUSTERED MIMO CHANNELS

We first compute the spatial correlation coefficients of CPAs in closed-form for multi-cluster channel models. From these coefficients, we analytically derive a lower bound on the MIMO ergodic capacity and demonstrate that the CPA performance can be evaluated over a reduced set of channel parameters with minimal error. This result is used to simplify the proposed optimization algorithm, yielding a significant reduction in computational complexity.

¹For the rest of this paper, we denote the bottom patch in Fig. 1 with “1” and the top patch with “2”.

A. Spatial Correlation of CPAs in Multi-Cluster Channels

In narrowband systems, the spatial correlation between the ℓ -th and m -th antennas of the MIMO array can be expressed as

$$r_{\ell,m} = \frac{1}{N_c} \sum_{i=1}^{N_c} r_{\ell,m}^{(i)} \quad (3)$$

where $r_{\ell,m}^{(i)}$ is the correlation coefficient corresponding to the i -th cluster and the normalization factor before the summation is to satisfy the trace constraint of the spatial correlation matrix (i.e., $\text{Tr}(\mathbf{R}) = N$)². Moreover, $\ell, m = 1, \dots, N$, where N denotes the number of array elements at the transmitter or receiver, and we focus on the special case of $N = 2$.

In [11] we derived closed-form expressions of the correlation coefficients in single-cluster channels (i.e., $N_c = 1$). Now we compute analytically these correlation coefficients accounting for multiple clusters. To simplify this analysis we assume that the N_c clusters experience the same angle spread (i.e., $\sigma_{\phi}^{(i)} = \sigma_{\phi}$, $\forall i = 1, \dots, N_c$). Under this assumption, substituting equations (16) and (20) in [11] into (3), we derive the auto-correlation coefficient as

$$r_{1,1}(N_c, \Phi, \sigma_{\phi}) = \frac{|\alpha(\rho, n)|^2}{\left(1 - e^{-\sqrt{2}\pi/\sigma_{\phi}}\right)} \frac{(n\sigma_{\phi})^2}{1 + 2(n\sigma_{\phi})^2} \times \left[1 - e^{-\sqrt{2}\pi/\sigma_{\phi}} + \frac{1 - e^{-\sqrt{2}\pi/\sigma_{\phi}} \cos(n\pi)}{N_c(n\sigma_{\phi})^2} \sum_{i=1}^{N_c} \cos^2(n\phi_c^{(i)}) \right] \quad (4)$$

and the cross-correlation coefficient as

$$r_{1,2}(N_c, \Phi, \sigma_{\phi}) = \frac{|\alpha(\rho, n)|^2}{2N_c [1 + 2(n\sigma_{\phi})^2]} \sum_{i=1}^{N_c} \sin(2n\phi_c^{(i)}), \quad (5)$$

respectively. Note that the auto-correlation coefficient for the second patch is derived from equation (4), accounting for the angle shift (ϕ_0) across the two antennas, and $r_{2,2}(\phi_c, \sigma_{\phi}) = r_{1,1}(\phi_c - \phi_0, \sigma_{\phi})$. Moreover, the cross-correlation coefficient $r_{2,1}$ has the same expression as (5).

B. Eigenvalue Analysis

The eigenvalues $\lambda_{(1,2)}$ of the 2×2 spatial correlation matrix (\mathbf{R}) are computed using the well-known quadratic equation as

$$\begin{aligned} \lambda_{(1,2)} &= \lambda_{(1,2)}(N_c, \Phi, \sigma_{\phi}) \\ &= \frac{1}{2} \left[(r_{1,1} + r_{2,2}) \pm \sqrt{4r_{1,2}r_{2,1} + (r_{1,1} - r_{2,2})^2} \right] \end{aligned} \quad (6)$$

where λ_1 and λ_2 are the maximum and minimum eigenvalues of spatial correlation matrix \mathbf{R} , respectively. The eigenvalues in (6) depend on the channel parameters (i.e., N_c , Φ and σ_{ϕ}) through the spatial correlation coefficients in (4) and (5). Hereafter, we derive bounds on these eigenvalues for CPAs, assuming the mode number n is even. Analogous results can be easily derived for n odd, by using similar approximation as in equation (30) in [11].

²We use $\text{Tr}(\cdot)$ to denote the trace of a matrix.

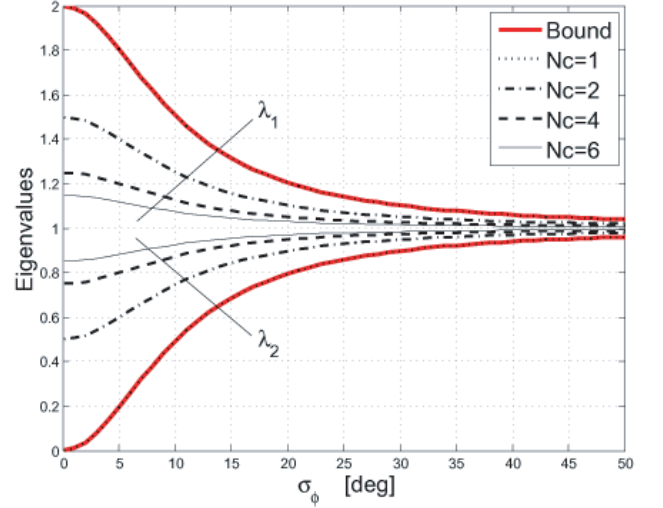


Fig. 3. Exact eigenvalues (λ_1 and λ_2) and bounds in (9) and (10). The channel is simulated with variable N_c , mean AoAs generated as $\phi_c^{(i)} = \tilde{\phi}(i-1)/N_c$ (with $i = 1, \dots, N_c$ and $\tilde{\phi} = 120^\circ$) and variable AS (σ_{ϕ}).

We expand the two terms in (6) within the brackets by substituting the correlation coefficients in (4) and (5), and obtain (7) and

$$\begin{aligned} &4r_{1,2}r_{2,1} + (r_{1,1} - r_{2,2})^2 \stackrel{(n \text{ even})}{=} \left[\frac{|\alpha(\rho, n)|^2}{1 + 2(n\sigma_{\phi})^2} \right]^2 \\ &\times \left\{ \left[\frac{1}{N_c} \sum_{i=1}^{N_c} \cos(2n\phi_c^{(i)}) \right]^2 + \left[\frac{1}{N_c} \sum_{i=1}^{N_c} \sin(2n\phi_c^{(i)}) \right]^2 \right\} \\ &\leq \left[\frac{|\alpha(\rho, n)|^2}{1 + 2(n\sigma_{\phi})^2} \right]^2. \end{aligned} \quad (8)$$

Note that the upper bound in (8) follows from the inequalities $\cos y \leq 1$ and $\sin y \leq 1$, $\forall y \in [0, 2\pi)$.

Substituting (7) and (8) into (6) we derive bounds on the eigenvalues of the CPA as

$$\lambda_1(\sigma_{\phi}) \leq 1 + \frac{1}{1 + 2(n\sigma_{\phi})^2} \quad (9)$$

$$\lambda_2(\sigma_{\phi}) \geq 1 - \frac{1}{1 + 2(n\sigma_{\phi})^2}. \quad (10)$$

In Fig. 3 we compare the bounds on λ_1 and λ_2 against their exact expressions as a function of the cluster AS for different values of N_c . The mean AoAs are generated as $\phi_c^{(i)} = \tilde{\phi}(i-1)/N_c$ (with $i = 1, \dots, N_c$ and $\tilde{\phi} = 120^\circ$) and variable AS (σ_{ϕ}). Fig. 3 shows that the bounds in (9) and (10) are close to the exact expression of the eigenvalues in (6) for $\sigma_{\phi} > 15^\circ$, which is also the lowest value of AS defined by the IEEE 802.11n standard channel model [34] for practical indoor propagation environments. Note that the equalities in (9) and (10) hold with equality only for the single cluster case, as shown in Fig. 3.

C. Lower Bound on the MIMO Ergodic Capacity

In Section II-A we showed that clustered channel models are defined by a large set of parameters. Optimizing the

$$\begin{aligned}
r_{1,1} + r_{2,2} &= \frac{|\alpha(\rho, n)|^2}{\left(1 - e^{-\sqrt{2}\pi/\sigma_\phi}\right)} \frac{(n\sigma_\phi)^2}{1 + 2(n\sigma_\phi)^2} \\
&\times \left[2 \left(1 - e^{-\sqrt{2}\pi/\sigma_\phi}\right) + \frac{1 - e^{-\sqrt{2}\pi/\sigma_\phi} \cos(n\pi)}{N_c(n\sigma_\phi)^2} \sum_{i=1}^{N_c} \left[\cos^2(n\phi_c^{(i)}) + \sin^2(n\phi_c^{(i)}) \right] \right] \\
&= \frac{|\alpha(\rho, n)|^2}{\left(1 - e^{-\sqrt{2}\pi/\sigma_\phi}\right)} \frac{(n\sigma_\phi)^2}{1 + 2(n\sigma_\phi)^2} \left[2 \left(1 - e^{-\sqrt{2}\pi/\sigma_\phi}\right) + \frac{1 - e^{-\sqrt{2}\pi/\sigma_\phi} \cos(n\pi)}{(n\sigma_\phi)^2} \right] \\
&\stackrel{(n \text{ even})}{=} |\alpha(\rho, n)|^2
\end{aligned} \tag{7}$$

design of 2-CPAs over many channel parameters to account for different propagation conditions would be computationally expensive. In this subsection we present a simple lower bound on the MIMO ergodic capacity expressed as a function of a reduced set of channel parameters. We show this bound corresponds to the capacity of single-cluster channels. We use this bound to optimize CPA designs with respect to the worst case scenario (single-cluster case), thereby reducing the computational complexity of the optimization algorithm. We observe that in the Kronecker model (1) the transmit and receive spatial correlations are treated separately. Since our goal is to optimize CPAs either at the transmit or receive side, without loss of generality, we consider single-sided spatially correlated channel models to simplify our analysis.

A tight lower bound on the MIMO ergodic capacity for zero-mean single-sided (only at the receiver) spatially correlated channels, assuming the model in (1) with $N_r \leq N_t$, was proposed in equation (82) in [39]

$$C \geq p \log \left[1 + \frac{\gamma_o}{N_t} \exp \left(\frac{1}{p} \left(\sum_{t=0}^{p-1} \psi(q-t) + \ln |\mathbf{R}| \right) \right) \right] \tag{11}$$

where $p = \min(N_r, N_t)$, $q = \max(N_r, N_t)$, γ_o is the average signal-to-noise ratio (SNR) and $\psi(\cdot)$ is the Euler Digamma function [39]. For the case of $N_r = N_t = 2$, equation (11) simplifies as

$$C \geq 2 \log \left[1 + \frac{\gamma_o}{2} \exp \left(\frac{\psi(1) + \psi(2)}{2} \right) \sqrt{|\mathbf{R}|} \right]. \tag{12}$$

Next, we use the following theorem to derive a lower bound on the ergodic capacity expressed as a function of channel and antenna parameters.

Theorem. Consider the eigenvalues λ_1 and λ_2 of \mathbf{R} , with $\lambda_1 \geq \lambda_2 \geq 0$ and $\text{Tr}(\mathbf{R}) \triangleq \lambda_1 + \lambda_2 = 2$ by definition. Assume $\lambda_1 \leq 1 + 1/[1 + 2(n\sigma_\phi)^2]$ as in (9). Then

$$|\mathbf{R}| \triangleq \lambda_1 \lambda_2 \geq 1 - \frac{1}{[1 + 2(n\sigma_\phi)^2]^2}. \tag{13}$$

Proof: see Appendix.

In (13) we defined n the mode number (assumed to be even) and σ_ϕ the cluster angle spread (assumed to be the same for all the clusters in the channel). Substituting (13) into (12) we obtain the following lower bound on the ergodic capacity of clustered MIMO channels with CPAs

$$C \geq 2 \log \left[1 + \frac{\gamma_o}{2} \exp \left(\frac{\psi(1) + \psi(2)}{2} \right) \sqrt{1 - \frac{1}{[1 + 2(n\sigma_\phi)^2]^2}} \right]. \tag{14}$$

Note that the equality in (13) holds for the single-cluster case as shown in equation (35) in [11]. Hence, the expression in (14) is the exact MIMO ergodic capacity for CPAs in single-cluster channels. Moreover, it is possible to verify through Monte Carlo simulations that the lower bound in (14) is close to the capacity achieved for $N_c = 6$ (i.e., rich scattering environment as defined in [34]).

These results demonstrate that the capacity of CPAs in single-cluster channels (i.e., $N_c = 1$) is always lower than the capacity obtained for $N_c > 1$ (for given value of AS). Hence, the proposed optimization method considers only the case of $N_c = 1$ to evaluate the performance of CPAs in clustered channels with minimal error and reduced computational complexity.

IV. MIMO COMMUNICATION PERFORMANCE METRICS

In this section, we first present a new definition of spatial correlation, particularly suitable for studies on pattern diversity. Then, we employ this definition to numerically compute the capacity performance of CPAs in different propagation scenarios as a function of the antenna parameters. Finally, we propose two MIMO communication performance metrics that will define the objective function of the proposed optimization algorithm.

A. Normalized Spatial Correlation

The general definition of spatial correlation between the ℓ -th and m -th elements of MIMO arrays is given by [40], [41]

$$r_{\ell,m} = \frac{\int_{4\pi} S(\Omega) \underline{E}_\ell(\Omega) \underline{E}_m^*(\Omega) d\Omega}{\left[\int_{4\pi} S(\Omega) |\underline{E}_\ell(\Omega)|^2 d\Omega \int_{4\pi} S(\Omega) |\underline{E}_m(\Omega)|^2 d\Omega \right]^{1/2}} \tag{15}$$

where $\Omega = (\phi, \theta)$ is the solid angle, $S(\Omega)$ is the PAS of the scattered fields, $\underline{E}_\ell(\Omega)$ is the far-field of the ℓ -th antenna of the CPA and $\ell, m \in \{1, 2\}$. Equation (15) can be simplified as in [42], by using the following normalization [4]

$$\int_{4\pi} S(\Omega) |\underline{E}_\ell(\Omega)|^2 d\Omega = 1. \tag{16}$$

The normalization in (16), however, holds only when either $S(\Omega)$ is uniformly distributed over the domain of integration or the antennas are characterized by isotropic radiation patterns.

In the most general case of ‘‘clustered’’ channel models (where the scattered energy is concentrated around the mean AOA of the clusters) and no isotropic antenna radiation

patterns (as for antenna designs that exploit pattern diversity), equation (16) is not satisfied for any channel condition, since the antenna gain may vary as a function of the clusters mean AOA. Then, we define a new spatial correlation coefficient as

$$r_{\ell,m} = \frac{\int_{4\pi} S(\Omega) \underline{E}_{\ell}(\Omega) \underline{E}_m^*(\Omega) d\Omega}{\int_{4\pi} S(\Omega) |\underline{E}_{\text{iso}}(\Omega)|^2 d\Omega} \quad (17)$$

where $\underline{E}_{\text{iso}}(\Omega)$ is the far-field of ideal isotropic radiators and $\ell, m \in \{1, 2\}$. Note that the envelope of (17) is not guaranteed to be lower than one, as for the conventional definition of correlation in (15), since the spatial correlation is normalized with respect to the antenna gain of ideal isotropic radiators. This normalization is introduced to take into account not only the cross-correlation, but also the effect of the antenna gain of non-isotropic radiators on the performance of MIMO arrays in clustered channels. The effect of the normalization in (17) on the capacity of MIMO systems exploiting pattern diversity will be studied in the following subsection.

Moreover, we assume

$$\int_{4\pi} S(\Omega) d\Omega = \int_{4\pi} |\underline{E}_{\text{iso}}(\Omega)|^2 d\Omega = \int_{4\pi} |\underline{E}_{\ell}(\Omega)|^2 d\Omega = 1 \quad (18)$$

where the first term of the equality is the condition for $S(\Omega)$ to be a p.d.f., whereas the last two equalities define the transmit power constraint. Consistent with the measurement results in [35], we assume the PAS over the θ angles is independent from the ϕ angles and most of the scattered energy propagates over the azimuth directions. Then, we write $S(\Omega) = P(\phi - \phi_c) \delta(\theta - \pi/2)$, where ϕ_c is the mean AOA of the cluster and $P(\phi)$ is generated according to the truncated Laplacian distribution in [43].

In the previous section we derived the closed-form expression of the auto- and cross-correlation coefficients of CPAs assuming ideal radiation patterns. In practical designs, however, near-field effects may produce pattern distortion and affect the performance of CPAs. Hereafter, we evaluate (17) numerically by employing realistic antenna radiation patterns computed with FEKO, an EM software tool based on the method of moments.

B. CPA Performance in Clustered MIMO Channels

We evaluate the MIMO capacity of different CPA designs as a function of the channel characteristics, by varying the physical parameters of the circular patch antennas. Different closed-form exact expressions of the MIMO ergodic capacity (with equal power allocation across the transmit antennas) for spatially correlated channels modeled as in (1) were proposed in [44], [45]. Here, we compute the capacity in [44] by using our proposed definition of spatial correlation in (17). Our goal is to evaluate the performance of CPAs employed either at the transmit or receive sides, thus we assume only single-sided (only at the receiver) spatially correlated channels. Moreover, we consider only single-cluster channels, for the reason explained in subsection III-C.

Fig. 4 depicts the MIMO ergodic capacity of the CPA as a function of the cluster mean AOA (ϕ_c) and per-cluster angle

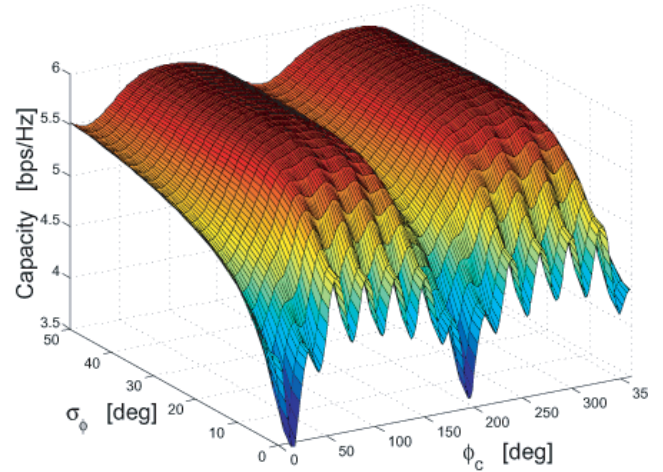


Fig. 4. Ergodic capacity of the CPA as a function of the cluster mean AOA (ϕ_c) and per-cluster AS (σ_ϕ), with $SNR = 10$ dB, $\rho_o = 0.45\lambda$ and $\rho_f = 0.64\rho_o$.

spread (σ_ϕ), with $SNR = 10$ dB. The CPA is simulated with parameters $\rho_o = 0.45\lambda$ and $\rho_f = 0.64\rho_o$, $h = 1.575$ mm and $\epsilon_r = 2.2$ to excite mode 3. The radiation patterns of the two antenna elements of the CPA evaluated through FEKO are given in Fig. 5(b). We observe that the capacity in Fig. 4 increases as a function of the AS and saturates to its maximum value for $\sigma_\phi > 15^\circ$ at any value of ϕ_c . Moreover, the capacity varies with respect to the mean AOA, unlike the theoretical results presented in [11]. These oscillations are due to the irregularity of the antenna radiation patterns in Fig. 5(b) (produced by near-field effects), and the notches in the capacity curve occur at the angles $\phi_c = 15^\circ, 195^\circ$ due to the reduced power radiated towards those angular directions.

Next, we evaluate the CPA performance with different antenna parameters. We consider three values of radius of the circular microstrip antennas: $\rho_o = 0.39\lambda, 0.45\lambda, 0.51\lambda$. In Fig. 5 we observe that, by varying the radius ρ_o and for fixed frequency of operation (i.e., 2.4 GHz as for WLANs), the shape and gain of the antenna radiation patterns vary. The value of $\rho_o = 0.45\lambda$ corresponds to the resonant frequency for mode 3 (with $h = 1.575$ mm and $\epsilon_r = 2.2$) as shown in subsection II-B. We observe that the patterns in Fig. 5(b) are irregular due to mutual coupling effects, unlike the ideal radiation pattern shown in [11] for mode 3. Moreover, by varying the radius ρ_o for fixed carrier frequency, it is not possible to excite mode 3 in the circular microstrip anymore, consistent to equation (7) in [11]. As a result, for $\rho_o = 0.39\lambda$ the antenna gains are lower than ideal isotropic radiators, while for $\rho_o = 0.51\lambda$ all the energy is radiated in two opposite spatial directions.

The effect of these radiation patterns on the systems performance is shown in Fig. 6, where we plot the MIMO ergodic capacity as a function of ϕ_c for the three values of ρ_o above. In the same figure we plot also the “ideal” MIMO capacity derived in i.i.d. channels, as reference. We note that the best performance is achieved for $\rho_o = 0.45\lambda$ due to the effect of pattern diversity, whereas for $\rho_o = 0.51\lambda$ the capacity reaches its maximum only in those spatial direction with high antenna gain. Note that the capacity produced by the CPAs may be

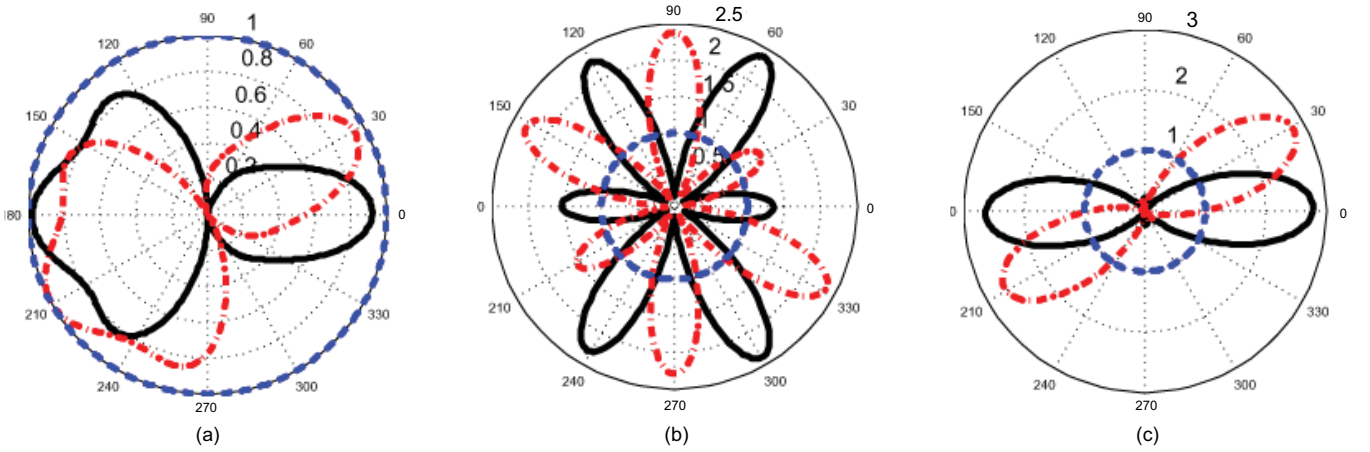


Fig. 5. Radiation patterns (over the azimuth plane) of the two elements of the CPA for different values of physical radius ρ_o , with $\rho_f = 0.64\rho_o$. Legend: antenna 1 (solid line); antenna 2 (dash-dot line); ideal isotropic radiator (dotted line).

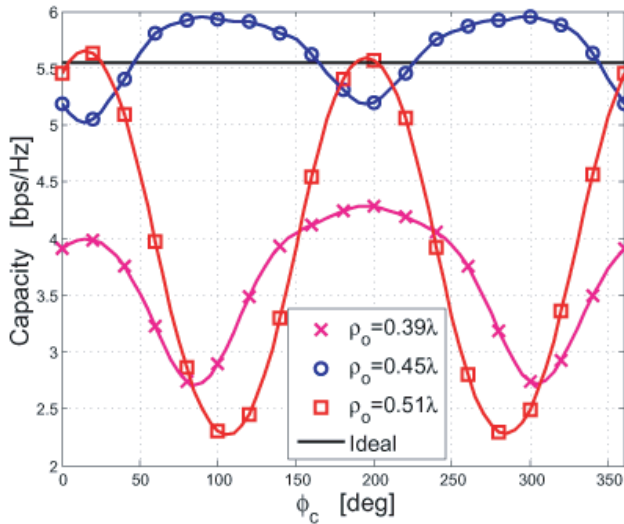


Fig. 6. Ergodic capacity of the CPA as a function of the cluster mean AOA, with $\sigma_\phi = 20^\circ$ and $SNR = 10$ dB.

higher than the ideal capacity due to the power normalization in (17) with respect to the gain of isotropic radiators, that accounts for both cross-correlation and antenna gain effects. Here, the physical interpretation of “ideal” performance can be described as the capacity achievable by two ideal isotropic radiators spaced apart at distance much greater than the wavelength (i.e., ideal array exploiting space diversity).

These results reveal that the CPA performance in realistic clustered MIMO channels is in fact sensitive to the antenna parameters. Moreover, we computed the CPA performance only in the worst case scenario of single-cluster channels, since that yields the lowest capacity values as proved in subsection III-C. Note that, we do account for different values of mean AOA and we aim to optimize CPA designs statistically, rather than in single propagation scenario. For example, the antenna solution in Fig. 5(c) outperforms the one in Fig. 5(b) only for certain values of mean AOA (i.e., $\sim 15^\circ$ and $\sim 195^\circ$) as shown in Fig. 6, due to larger gain towards those directions. The antenna (b), however, performs better than (c) as average and we prefer that design for its robustness in a variety of

propagation conditions. Based on these observations, hereafter we define two metrics to evaluate the statistical performance of CPAs in single-cluster channels, that will be used in the proposed optimization algorithm.

C. Performance Metrics for Optimization Algorithms

One common metric to evaluate the performance of MIMO arrays exploiting pattern diversity is the *inner product* of the antenna radiation patterns [40], [41], [46]

$$\Upsilon(\mathbf{x}) = \langle \underline{E}_\ell(\mathbf{x}), \underline{E}_m(\mathbf{x}) \rangle = \frac{\int_{4\pi} \underline{E}_\ell(\mathbf{x}; \Omega) \underline{E}_m^*(\mathbf{x}; \Omega) d\Omega}{\left[\int_{4\pi} |\underline{E}_\ell(\mathbf{x}; \Omega)|^2 d\Omega \int_{4\pi} |\underline{E}_m(\mathbf{x}; \Omega)|^2 d\Omega \right]^{1/2}}. \quad (19)$$

This metric is derived from (15) under the simplistic assumption of uniform distribution of the multipaths (i.e., $S(\Omega)$ has uniform p.d.f.). It is well known that the assumption of uniformly distributed PAS is not realistic and overestimates the MIMO channel capacity [47]. In realistic clustered channel environments, the MIMO ergodic capacity is a function of the cluster mean AOA and AS, as shown in Fig. 4. To solve the optimization algorithm for MIMO arrays, however, it is desirable to remove the dependence of the objective function on the channel parameters and express it only as a function of the antenna physical characteristics, as for the metric in (19). Hence, we propose two performance metrics derived from the ergodic capacity that are independent on the channel parameters and measure the statistical performance of MIMO arrays in clustered channels.

We denote with $C(\mathbf{x}; \phi_c, \sigma_\phi)$ the ergodic capacity as a function of the channel parameters for given CPA design described by \mathbf{x} . We define the *mean capacity* (\bar{C}) as

$$\bar{C}(\mathbf{x}) = \mathcal{E}_{\phi_c, \sigma_\phi} \{ C(\mathbf{x}; \phi_c, \sigma_\phi) \} = \int_0^{2\pi} \int_0^{2\pi} C(\mathbf{x}; \phi_c, \sigma_\phi) f_{\phi_c, \sigma_\phi}(\phi_c, \sigma_\phi) d\phi_c d\sigma_\phi \quad (20)$$

where $f_{\phi_c, \sigma_\phi}(\cdot)$ is the joint p.d.f. of ϕ_c and σ_ϕ , and we assume ϕ_c and σ_ϕ are independent and with uniform distributions, that is reasonable assumption for practical channel models. The

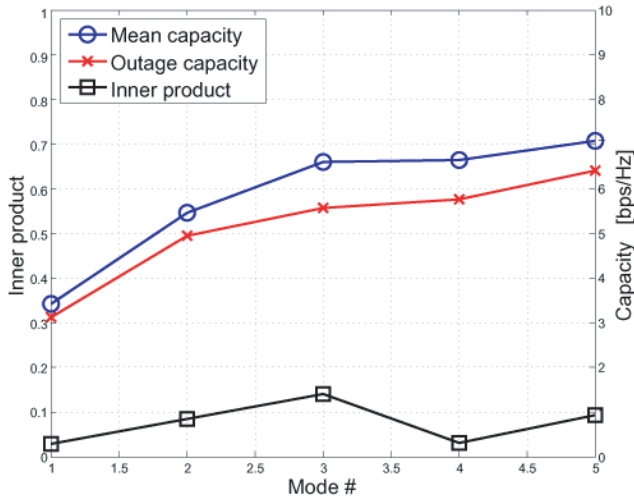


Fig. 7. Comparison of different metrics to evaluate the performance of pattern diversity.

mean capacity measures the average performance of the array in different propagation scenarios. Additionally, it is desirable to account for the notches in the capacity curve in Fig. 4, by introducing a notion of “outage”. We define the 10% *outage capacity* ($C_{10\%}$) as

$$\begin{aligned}
 & P[C(\mathbf{x}; \phi_c, \sigma_\phi) \leq C_{10\%}(\mathbf{x})] \\
 &= \int_0^{C_{10\%}(\mathbf{x})} C(\mathbf{x}; \phi_c, \sigma_\phi) f_{\phi_c, \sigma_\phi}(\phi_c, \sigma_\phi) d\phi_c d\sigma_\phi = 10\%
 \end{aligned} \quad (21)$$

where P denotes the probability of a random variable. Note that the ergodic capacity $C(\mathbf{x}; \phi_c, \sigma_\phi)$ in (20) and (21) is numerically evaluated through the closed-form expression in equation (46) in [44] and using the definition of spatial correlation in (17).

Fig. 7 compares the three metrics mentioned above: the mean capacity in (20), the 10% outage capacity in (21) and the conventional envelope of the inner product in (19). The circular patch antennas are simulated through FEKO with $\rho_f = 0.8\rho_o$, $h = 1.575$ mm and $\epsilon_r = 6$. Different values of radius are considered $\rho_o = 0.12\lambda, 0.2\lambda, 0.29\lambda, 0.36\lambda, 0.44\lambda$ to excite modes $n = 1, 2, 3, 4, 5$, respectively, at 2.4 GHz carrier frequency. Note that some values of ρ_o are slightly different from the theoretical ones reported in [48] due to near-field effects between the two antenna elements of the CPA.

In Fig. 7 it is possible to see that both mean and outage capacity increase as a function of the mode number due to the beneficial effect of pattern diversity, consistently to the theoretical results presented in [11]. Fig. 7 shows a large capacity gain (about 100%) between mode 1 and mode 5, revealing that careful design of the antenna radiation patterns is necessary for MIMO arrays that exploit pattern diversity in realistic clustered propagation channels. We observe that all five antenna designs in Fig. 7 resonate at the carrier frequency of operation, but provide different capacity values. This result reveals that array performance metrics from microwave theory (i.e., return loss) and communication theory (i.e., capacity) are not necessarily related, and their joint optimization is required for CPA designs in clustered channel models. Moreover, the

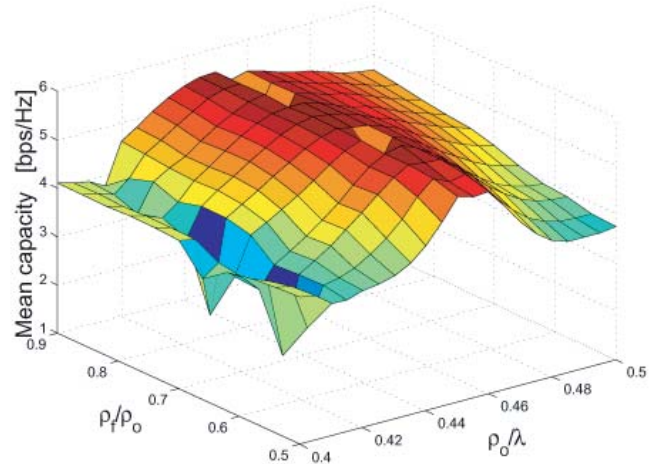


Fig. 8. Mean capacity in (20) as a function of the physical radius (ρ_o) and the feed location (ρ_f). The two antennas of the CPA are designed with physical parameters $h = 1.575$ mm and $\epsilon_r = 6$.

inner product in (19) oscillates around the value of 0.1, since the radiation patterns are orthogonal for any mode number. This result demonstrates that (20) and (21) are better measures of the effect of pattern diversity on systems performance, in realistic clustered MIMO channels, than the conventional inner product (19).

Finally, we compute the metrics in (20) and (21) as a function of the antenna parameters. Fig. 8 shows the mean capacity in (20) versus radius (ρ_o) and feeding location (ρ_f) of the circular microstrip antennas (with $h = 1.575$ mm and $\epsilon_r = 2.2$). It is possible to see that the maximum is reached for $\rho_o \approx 0.45\lambda$ for most of the values of ρ_f . The metrics in (20) and (21) will be used in the optimization algorithm to determine the best values of antenna parameters on the communication theoretic point of view.

V. MICROWAVE THEORY PERFORMANCE METRICS

Hereafter, we present different metrics from microwave theory used to evaluate the efficiency of CPA designs as a function of the physical antenna parameters.

A. S-parameters

The antenna efficiency depends on the losses at the input or within the structure of an antenna, and indicates the amount of radiated power for given input power [37]. The antenna efficiency is generally measured in terms of return loss or S_{11} and S_{22} scattering parameters, for 2-port antenna designs. Typical target value used to measure the bandwidth of S_{11} and S_{22} is -10 dB.

Due to the proximity of the two circular patch antennas, the performance of the CPA may be affected by mutual coupling effects. Mutual coupling results in distortion of the antenna radiation patterns [49]–[53] and power loss [54]–[56]. The effect of pattern distortion on the MIMO channel capacity was shown in Section IV-B. Power loss due to mutual coupling is generally measured in terms of the S_{12} and S_{21} scattering parameters, for 2-element arrays. The target value for the bandwidth of S_{12} and S_{21} is -20 dB.

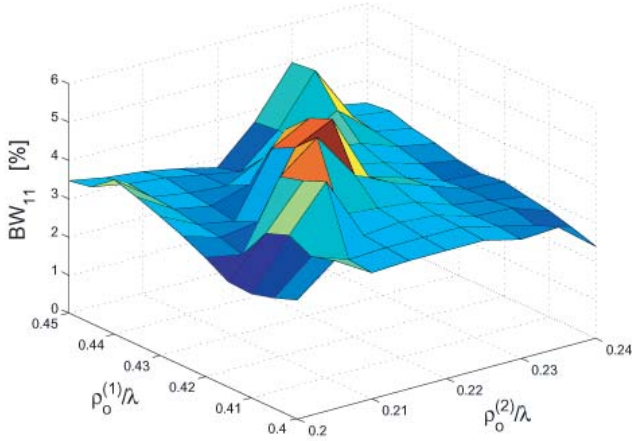


Fig. 9. Bandwidth BW_{11} as a function of the radii $\rho_o^{(1)}$ and $\rho_o^{(2)}$ of the two patch antennas of the CPA. The antenna parameters are: $\rho_f^{(1)} = 0.9\rho_o^{(1)}$, $h^{(1)} = 9$ mm, $\epsilon_r^{(1)} = 2.2$, $\rho_{gp}^{(1)} = 2\rho_o^{(1)}$, $\rho_f^{(2)} = 0.8\rho_o^{(2)}$, $h^{(2)} = 7$ mm, $\epsilon_r^{(2)} = 8$, $\rho_{gp}^{(2)} = 1.8\rho_o^{(2)}$.

B. Performance Metrics for Optimization Algorithms

The values of the S-parameters, expressed as a function of the frequency, depend on the physical characteristics of the antennas. To optimize the physical parameters of CPA designs we employ the bandwidth BW_{11} and BW_{22} defined as the measure of the set of frequencies for which $|S_{11}|$ and $|S_{22}|$ are below -10 dB, respectively. Similarly, BW_{12} and BW_{21} denote the bandwidth of $|S_{12}|$ and $|S_{21}|$, respectively, for the target -20 dB.

Fig. 9 depicts the bandwidth BW_{11} as a function of the radii $\rho_o^{(1)}$ and $\rho_o^{(2)}$ of the two patches. The bandwidth is expressed in percentage value with respect to the carrier frequency $f_c = 2.44$ GHz for WLANs and is measured within the frequency band $[2.2, 2.7]$ GHz. Moreover, the substrate of the bottom and top patches are characterized by $\epsilon_r^{(1)} = 2.2$ and $\epsilon_r^{(2)} = 8$, respectively. We observe that BW_{11} reaches values of $\sim 5\%$ for $\rho_o^{(1)} \approx 0.42\lambda$ and $\rho_o^{(2)} \approx 0.22\lambda$. These are the values of radius for which the two patch antennas resonate with mode 3 for the given values of ϵ_r , similarly to the theoretical results in [48].

Note that the bandwidth of the circular patch antennas is also a function of the substrate height h and dielectric constant ϵ_r , feed location ρ_f and size of the ground plane ρ_{gp} as shown in [26], [37]. To optimize the CPA design over these physical parameters we formulate a multidimensional optimization algorithm as in the following section.

VI. OPTIMIZATION ALGORITHM FOR 2-CPA DESIGNS

So far, we studied the performance of CPA designs as a function of the antenna parameters and defined different metrics. Here, we present an algorithm to optimize the performance of CPAs by jointly maximizing performance metrics from communication theory (i.e., MIMO channel capacity) and microwave theory (i.e., bandwidth).

A. Algorithm Description and Results

In Section IV we showed there are cases where different MIMO array designs yield similar capacity performance with

different S-parameters. For example, Fig. 6 shows that the antenna designs in Fig. 5(b) and Fig. 5(c) yield similar capacity (close to the ideal case) for certain values of mean AOA (i.e., $\sim 15^\circ$ and $\sim 195^\circ$). The solution (c), however, has large return loss as opposed to (b), that is designed to resonate at 2.4 GHz. Note that the large capacity gain for (c) is only due to the very directional radiation patterns. On the other hand, Fig. 7 depicts the capacity performance of five CPAs resonating at 2.4 GHz with different modes, but we observe that the capacity performance varies with the mode number. Hence, the S-parameters and capacity metrics may not be correlated. Motivated by these results, here we present an algorithm for MIMO arrays that jointly optimizes communication theory and microwave theory performance metrics.

In Fig. 8 we showed that mean and outage capacity of the CPA vary as a function of \mathbf{x} . Here, we define the objective function of the optimization algorithm based on *MIMO communication performance* as

$$g_{\text{MIMO}}(\mathbf{x}) = w_1 \overline{C}(\mathbf{x}) + w_2 C_{10\%}(\mathbf{x}) \quad (22)$$

where w_1 and w_2 are weighting values. Note that the values of w_1 and w_2 can be chosen depending on whether the design has to be optimized with respect to average or outage performance.

Similarly, Fig. 9 shows the antenna bandwidth is also a function of \mathbf{x} . We denote the bandwidth of the scattering parameter S_{ij} as $BW_{ij}(\mathbf{x}) = |[\underline{f}_{ij}(\mathbf{x}), \overline{f}_{ij}(\mathbf{x})]|$, where $|\cdot|$ is the measure of a set and \underline{f}_{ij} and \overline{f}_{ij} characterize the range of frequencies that satisfy the predefined target (i.e., -10 dB for S_{11} and S_{22} , -20 dB for S_{12} and S_{21}). Moreover, we define $\mathcal{BW} = [\underline{f}, \overline{f}]$ as the target frequency band. For designs conceived for WLANs applications, we assume $\mathcal{BW} = [2.4, 2.48]$ GHz. With these definitions, we write the *microwave theory performance* metric as

$$g_{\text{MW}}(\mathbf{x}) = I_{A_{11}}(\mathbf{x}) I_{A_{22}}(\mathbf{x}) I_{A_{12}}(\mathbf{x}) I_{A_{21}}(\mathbf{x}) - 1 \quad (23)$$

where $A_{ij} = \{\mathbf{x} | \underline{f}_{ij}(\mathbf{x}) \leq \underline{f}, \overline{f}_{ij}(\mathbf{x}) \geq \overline{f}\}$ and $I_{A_{ij}}(\cdot)$ denotes the indicator function³.

The goal of the proposed optimization algorithm is to determine the CPA design that provides statistically the best capacity performance in correlated channels, while satisfying predefined target bandwidth requirements. Hence, we use (22) as objective function and (23) to define the (non-linear) equality constraint, and formulate the optimization problem as

$$\mathbf{x}^{\text{opt}} = \arg \max_{\mathbf{x} \in \mathcal{X}} \{g_{\text{MIMO}}(\mathbf{x}) | g_{\text{MW}}(\mathbf{x}) = 0\} \quad (24)$$

where the feasible set is given by

$$\mathcal{S} = \{\mathbf{x} \in \mathcal{X} | g_{\text{MW}}(\mathbf{x}) = 0\}. \quad (25)$$

Finally, we solve the optimization problem in (24). We observe that the objective function in (22) is not convex, as shown in Fig. 8, and to solve (24) we use a genetic algorithm [18], [19], [57]. In our genetic algorithm the population size is 40 and the mutation rate is 50%. There are six optimization

³The indicator function is defined as

$$I_A(y) = \begin{cases} 1 & \text{if } y \in A; \\ 0 & \text{otherwise.} \end{cases}$$

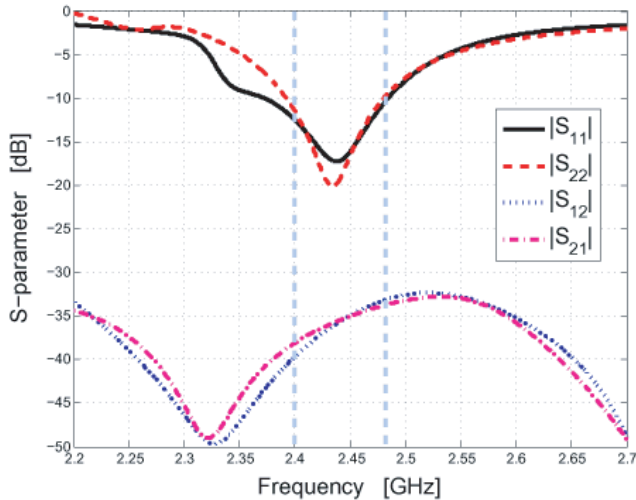


Fig. 10. S-parameters for the optimized CPA design with $\rho_o^{(1)} = 0.43\lambda$ and $\rho_o^{(2)} = 0.22\lambda$. The vertical dashed lines indicate the target bandwidth (\mathcal{BW}) used in the optimization algorithm.

parameters as in (2) for the two antennas of the CPA. These parameters are quantized over 6 bits, such that the chromosomes of the population consist of 36 bits total. Moreover, to evaluate (23) with low computational complexity, we calculate the S-parameters over the target frequency band by applying the Cauchy method [58]–[60].

We solve (24) through this genetic algorithm and find the antenna parameters that optimize the performance of the CPA: $\rho_o^{(1)} = 0.43\lambda$, $\rho_f^{(1)} = 0.9\rho_o^{(1)}$, $h^{(1)} = 9$ mm, $\rho_o^{(2)} = 0.22\lambda$, $\rho_f^{(2)} = 0.8\rho_o^{(2)}$ and $h^{(2)} = 7$ mm, where we fixed $\epsilon_r^{(1)} = 2.2$, $\rho_{gp}^{(1)} = 2\rho_o^{(1)}$, $\epsilon_r^{(2)} = 8$ and $\rho_{gp}^{(2)} = 1.8\rho_o^{(2)}$. With these parameters, mode 3 is excited for both the bottom and top patch antennas of the CPA. Fig. 10 shows the S-parameters for our proposed CPA design. We observe that the return loss $|S_{11}|$ and $|S_{22}|$ for the two ports of the CPA is below -10 dB within the target frequency band $\mathcal{BW} = [2.4, 2.48]$ GHz for WLANs. Similarly, the parameters $|S_{12}|$ and $|S_{21}|$ are way below -20 dB within \mathcal{BW} , revealing very good isolation between the two ports of the CPA.

B. Discussion on MIMO Antenna Synthesis

The analysis and results presented in this paper are derived for one specific MIMO antenna structure (i.e., CPAs). The metrics and optimization methodology presented in this contribution, however, can be generalized to any MIMO array solution that exploits pattern diversity.

The analysis described in Section III is restricted to CPAs. But similar results can be obtained for different antenna structures, as long as the electric field of the antennas can be expressed in closed form, similarly to equations (5) and (6) in [11] for CPAs. The new definition of spatial correlation in (17) can be used for any MIMO array exploiting pattern diversity and can be numerically evaluated from the electric field of the antennas. The capacity performance metrics defined in (20) and (21) can be used to optimize any MIMO array in clustered channels. Note that, similar metrics can be defined from the bit error rate (BER) closed form expressions

of MIMO bit-interleaved coded modulation (BICM) systems presented in [61]. Finally, the optimization algorithm proposed in subsection VI-A as well as the block diagram in Fig. 2 are general and can be used in any MIMO array synthesis problem. The entries of the vector \mathbf{x} in (2) and in Fig. 2, however, may need to be adjusted depending on the type of antenna structure to be optimized.

VII. CONCLUSIONS

We proposed a novel optimization methodology to design circular patch arrays (CPAs) exploiting pattern diversity in realistic clustered MIMO channels. This optimization methodology employs a combination of MIMO communication and microwave theory performance metrics. We first motivated the choice of the MIMO communication performance metrics through capacity analysis of CPAs in clustered channel models. Then we defined two MIMO communication performance metrics, expressed only as a function of the antenna parameters, to measure the mean and outage CPA performance in a variety of propagation scenarios. We also measured the performance of CPAs in terms of bandwidth and mutual coupling effects. Finally, we formulated and solved the optimization methodology producing the optimal CPA design. This novel optimization method was here presented for the particular case of CPAs, but can be extended to any kind of array type that uses pattern diversity in clustered MIMO channels. Future work include manufacturing and measurement validation of the optimal CPA design proposed in this paper.

APPENDIX

Proof of the Theorem:

Let us define

$$A \triangleq \frac{1}{1 + 2(n\sigma_\phi)^2} \quad (26)$$

and

$$\lambda_1 \triangleq 1 + B. \quad (27)$$

From (27) and by the hypothesis $\lambda_1 + \lambda_2 = 2$, we obtain

$$\lambda_2 = 1 - B. \quad (28)$$

Next, from (26), (27) and the hypothesis we derive $\lambda_1 \triangleq 1 + B \leq 1 + A$, that can be simplified as

$$B \leq A. \quad (29)$$

Finally, by using (27) and (28) and the property in (29), we derive

$$\lambda_1\lambda_2 = (1 + B)(1 - B) = 1 - B^2 \geq 1 - A^2. \quad (30)$$

REFERENCES

- [1] D.-S. Shiu, G. J. Foschini, M. J. Gans, and J. M. Kahn, "Fading correlation and its effect on the capacity of multielement antenna systems," *IEEE Trans. Commun.*, vol. 48, no. 3, pp. 502–513, Mar. 2000.
- [2] M. A. Jensen and J. W. Wallace, "A review of antennas and propagation for MIMO wireless communications," *IEEE Trans. Antennas Propagat.*, vol. 52, pp. 2810–2824, Nov. 2004.
- [3] A. Forenza and R. W. Heath Jr., "Impact of antenna geometry on MIMO communication in indoor clustered channels," in *Proc. IEEE Antennas and Prop. Symp.*, vol. 2, pp. 1700–1703, June 2004.

- [4] R. Vaughan, "Switched parasitic elements for antenna diversity," *IEEE Trans. Antennas Propagat.*, vol. 47, pp. 399–405, Feb. 1999.
- [5] C. B. D. Jr, K. Dietze, J. R. Nealy, and W. L. Stutzman, "Spatial, polarization, and pattern diversity for wireless handheld terminals," in *Proc. IEEE Antennas and Prop. Symp.*, vol. 49, pp. 1271–1281, Sept. 2001.
- [6] S. Visuri and D. T. Slock, "Colocated antenna arrays: design desiderata for wireless communications," in *Proc. Sensor Array and Multichannel Sign. Proc. Workshop*, pp. 580–584, Aug. 2002.
- [7] L. Dong, H. Ling, and R. W. Heath Jr., "Multiple-input multiple-output wireless communication systems using antenna pattern diversity," in *Proc. IEEE Glob. Telecom. Conf.*, vol. 1, pp. 997–1001, Nov. 2002.
- [8] L. Dong, H. Choo, H. Ling, and J. R. W. Heath, "MIMO wireless handheld terminals using antenna pattern diversity," *IEEE Trans. Wireless Commun.*, vol. 4, pp. 1869–1873, July 2005.
- [9] A. M. Tulino, S. Verdu, and A. Lozano, "Capacity of antenna arrays with space, polarization and pattern diversity," in *Proc. IEEE Info. Th. Workshop*, pp. 324–327, Mar. 2003.
- [10] P. Mattheijssen, M. H. A. J. Herben, G. Dolmans, and L. Leyten, "Antenna-pattern diversity versus space diversity for use at handhelds," *IEEE Trans. Veh. Technol.*, vol. 53, pp. 1035–1042, July 2004.
- [11] A. Forenza and R. W. Heath Jr., "Benefit of pattern diversity via 2-element array of circular patch antennas in indoor clustered MIMO channels," *IEEE Trans. Commun.*, vol. 54, pp. 943–954, May 2006.
- [12] V. Pohl, V. Jungnickel, T. Haustein, and C. von Helmolt, "Antenna spacing in MIMO indoor channels," in *Proc. IEEE Veh. Technol. Conf.*, vol. 2, pp. 749–753, May 2002.
- [13] M. Stoytchev, H. Safar, A. L. Moustakas, and S. Simon, "Compact antenna arrays for MIMO applications," in *Proc. IEEE Antennas and Prop. Symp.*, vol. 3, pp. 708–711, July 2001.
- [14] M. Wennström and T. Svantesson, "An antenna solution for MIMO channels: the switched parasitic antenna," in *Proc. IEEE Int. Symp. on Pers., Indoor and Mobile Radio Comm.*, vol. 1, pp. A–159–A–163, Sept. 2001.
- [15] C. Waldschmidt, S. Schulteis, and W. Wiesbeck, "Complete RF system model for analysis of compact MIMO arrays," *IEEE Trans. Veh. Technol.*, vol. 53, pp. 579–586, May 2004.
- [16] M. L. Morris and M. A. Jensen, "Network model for MIMO systems with coupled antennas and noisy amplifiers," *IEEE Trans. Antennas Propagat.*, vol. 53, pp. 545–552, Jan. 2005.
- [17] E. Altshuler, "Electrically small self-resonant wire antennas optimized using a genetic algorithm," *IEEE Trans. Antennas Propagat.*, vol. 50, no. 3, pp. 297–300, Mar. 2002.
- [18] H. Choo and H. Ling, "Design of multiband microstrip antennas using a genetic algorithm," *IEEE [see also IEEE Microwave and Guided Wave Letters] Microwave and Wireless Components Letters*, vol. 12, no. 9, pp. 345–347, Sept. 2002.
- [19] H. Choo, R. Rogers, and H. Ling, "Design of electrically small wire antennas using a pareto genetic algorithm," *IEEE Trans. Antennas Propagat.*, vol. 53, no. 3, pp. 1038–1046, Mar. 2005.
- [20] H. Delgado and M. Thorsby, "Automated synthesis of a printed dipole antenna with FD-TD and a novel artificial neural network," in *Proc. IEEE Antennas and Prop. Symp.*, vol. 4, June 2004, pp. 4400–4403.
- [21] B. Fischer, A. Yagle, and J. Volakis, "Electromagnetic optimization of a patch antenna over a textured substrate using total least squares," in *Proc. IEEE Antennas and Prop. Symp.*, vol. 4, June 2004, pp. 4428–4431.
- [22] R. Ayestarin, F. Las-Heras, and L. Herran, "Neural network-based pattern synthesis of array antennas with element specification," in *Proc. IEEE Antennas and Prop. Symp.*, vol. 1, June 2004, pp. 519–522.
- [23] D. Webb, "Base station design for sector coverage using a genetic algorithm with the method of moments," in *Proc. IEEE Antennas and Prop. Symp.*, vol. 4, June 2004, pp. 4396–4399.
- [24] A. M. Tulino, A. Lozano, and S. Verdu, "Impact of antenna correlation on the capacity of multiantenna channels," *IEEE Trans. Inform. Theory*, vol. 51, pp. 2491–2509, July 2005.
- [25] D. M. Pozar, *Microwave Engineering (second edition)*. New York: John Wiley and Sons, Inc., 1998.
- [26] S. Yano and A. Ishimaru, "A theoretical study of the input impedance of a circular microstrip disk antenna," *IEEE Trans. Antennas Propagat.*, vol. 29, pp. 77–83, Jan. 1981.
- [27] R. G. Vaughan, "Two-port higher mode circular microstrip antennas," *IEEE Trans. Antennas Propagat.*, vol. 36, pp. 309–321, Mar. 1988.
- [28] A. Forenza, F. Sun, and R. W. Heath Jr., "Pattern diversity with multi-mode circular patch antennas in clustered MIMO channels," in *Proc. IEEE Antennas and Prop. Symp.*, vol. 3B, pp. 438–441, July 2005.
- [29] J. P. Kermoal, L. Schumacher, K. I. Pedersen, P. E. Mogensen, and F. Frederiksen, "A stochastic MIMO radio channel model with experimental validation," *IEEE J. Select. Areas Commun.*, vol. 20, no. 6, pp. 1211–1226, Aug. 2002.
- [30] H. Özcelik, M. Herdin, W. Weichselberger, J. Wallace, and E. Bonek, "Deficiencies of 'Kronecker' MIMO radio channel model," *Electron. Lett.*, vol. 39, no. 16, pp. 1209–1210, Aug. 2003.
- [31] W. Weichselberger, H. Özcelik, M. Herdin, and E. Bonek, "A novel stochastic MIMO channel model and its physical interpretation," in *Proc. International Symposium on Wireless Personal Multimedia Communications, WPMC*, Yokosuka, Japan, Oct. 2003.
- [32] S. Wyne, A. F. Molisch, P. Almers, G. Eriksson, J. Karedal, and F. Tufvesson, "Statistical evaluation of outdoor-to-indoor office MIMO measurements at 5.2 GHz," in *Proc. IEEE Veh. Technol. Conf.*, vol. 1, pp. 146–150, July 2005.
- [33] C. Oestges, H. Özcelik, and E. Bonek, "On the practical use of analytical MIMO channel models," in *Proc. IEEE Antennas and Prop. Symp.*, vol. 3B, pp. 406–409, July 2005.
- [34] V. Erceg *et al.*, "TGN channel models," IEEE 802.11-03/940r4, May 2004.
- [35] L. M. Correia, *Wireless Flexible Personalised Communications*. New York: John Wiley and Sons, Inc., 2001.
- [36] R. G. Vaughan and J. B. Anderson, "A multiport patch antenna for mobile communications," in *Proc. 14th European Microwave Conf.*, pp. 607–612, 1984.
- [37] C. A. Balanis, *Antenna Theory: Analysis and Design (second edition)*. New York: John Wiley and Sons, Inc., 1982.
- [38] A. Paulraj, R. Nabar, and D. Gore, *Introduction to Space-Time Wireless Communications*. 40 West 20th Street, New York: Cambridge University Press, 2003.
- [39] M. R. McKay and I. B. Collings, "General capacity bounds for spatially correlated Rician MIMO channels," *IEEE Trans. Inform. Theory*, vol. 51, pp. 3121–3145, Sept. 2005.
- [40] R. G. Vaughan and J. B. Anderson, "Antenna diversity in mobile communications," *IEEE Trans. Veh. Technol.*, vol. VT-36, pp. 149–172, Nov. 1987.
- [41] M. A. Jensen and Y. Rahmat-Samii, "Performance analysis of antennas for hand-held transceivers using FDTD," *IEEE Trans. Antennas Propagat.*, vol. 42, pp. 1106–1113, Aug. 1994.
- [42] T. Svantesson, M. A. Jensen, and J. W. Wallace, "Analysis of electromagnetic field polarizations in multiantenna systems," *IEEE Trans. Wireless Commun.*, vol. 3, pp. 641–646, Mar. 2004.
- [43] Q. Spencer, M. Rice, B. Jeffs, and M. Jensen, "A statistical model for angle of arrival in indoor multipath propagation," in *Proc. IEEE Veh. Technol. Conf.*, vol. 3, pp. 1415–1419, May 1997.
- [44] M. Kiessling and J. Speidel, "Mutual information of MIMO channels in correlated Rayleigh fading environments—a general solution," in *Proc. IEEE Int. Conf. on Comm.*, vol. 2, pp. 814–818, June 2004.
- [45] A. Forenza, M. R. McKay, A. Pandharipande, R. W. Heath Jr., and I. B. Collings, "Adaptive MIMO transmission for exploiting the capacity of spatially correlated channels," *IEEE Trans. Veh. Technol.*, vol. 56, no. 2, pp. 619–630, Mar. 2007.
- [46] S. C. K. Ko and R. D. Murch, "Compact integrated diversity antenna for wireless communications," *IEEE Trans. Antennas Propagat.*, vol. 49, pp. 954–960, June 2001.
- [47] K.-H. Li, M. Ingram, and A. Van Nguyen, "Impact of clustering in statistical indoor propagation models on link capacity," *IEEE Trans. Commun.*, vol. 50, no. 4, pp. 521–523, 2002.
- [48] A. Forenza, G. Wan, and J. R. W. Heath, "Optimization of 2-element arrays of circular patch antennas in spatially correlated MIMO channels," *Proc. IEEE Int. Waveform Diversity and Design Conf.*, Jan. 2006.
- [49] M. Fakhereddin and K. Dandekar, "Combined effect of polarization diversity and mutual coupling on MIMO capacity," in *Proc. IEEE Antennas and Prop. Symp.*, vol. 2, pp. 495–498, June 2003.
- [50] T. Svantesson and A. Ranheim, "Mutual coupling effects on the capacity of multielement antenna systems," in *Proc. IEEE Int. Conf. Acoust., Speech and Sig. Proc.*, vol. 4, pp. 2485–2488, May 2001.
- [51] P. N. Fletcher, M. Dean, and A. R. Nix, "Mutual coupling in multi-element array antennas and its influence on MIMO channel capacity," *IEEE Electron. Lett.*, vol. 39, pp. 342–344, Feb. 2003.
- [52] V. Jungnickel, V. Pohl, and C. V. Helmolt, "Capacity of MIMO systems with closely spaced antennas," *IEEE Commun. Lett.*, vol. 7, pp. 361–363, Aug. 2003.
- [53] A. Konanur, K. Gosalia, S. Krishnamanhy, B. Hughes, and G. Lazzi, "Investigation of the performance of co-polarized, co-located electric and magnetic dipoles for increasing channel capacity," in *Proc. IEEE Antennas and Prop. Symp.*, vol. 2, pp. 531–534, June 2003.

- [54] J. W. Wallace and M. A. Jensen, "Termination-dependent diversity performance of coupled antennas: Network theory analysis," *IEEE Trans. Antennas Propagat.*, vol. 52, pp. 98–105, Jan. 2004.
- [55] R. R. Ramirez and F. D. Flaviis, "A mutual coupling study of linear and circular polarized microstrip antennas for diversity wireless systems," *IEEE Trans. Antennas Propagat.*, vol. 51, pp. 238–248, Feb. 2003.
- [56] I. Salonen, A. Toropainen, and P. Vainikainen, "Linear pattern correction in a small microstrip antenna array," *IEEE Trans. Antennas Propagat.*, vol. 52, pp. 578–586, Feb. 2004.
- [57] H. Choo and H. Ling, "Design of broadband and dual-band microstrip antennas on a high-dielectric substrate using a genetic algorithm," *IEEE Proc. Microwaves, Antennas and Propagation*, vol. 150, no. 3, pp. 137–142, June 2003.
- [58] K. Kottapalli, T. K. Sarkar, Y. Hua, E. K. Miller, and G. J. Burke, "Accurate computation of wide-band response of electromagnetic systems utilizing narrow-band information," *IEEE Trans. Microwave Theory Techniques*, vol. 39, no. 4, pp. 682–687, Apr. 1991.
- [59] R. S. Adve, T. K. Sarkar, S. M. Rao, E. K. Miller, and D. R. Pflug, "Application of the Cauchy method for extrapolating/interpolating narrowband system responses," *IEEE Trans. Microwave Theory Techniques*, vol. 45, pp. 837–845, May 1997.
- [60] Y. Kim, M. Gerwell, and H. Ling, "Application of the Cauchy method to genetic algorithms for broadband antenna design," in *Proc. IEEE Antennas and Prop. Symp.*, vol. 3, July 2005, pp. 590–593.
- [61] M. R. McKay, I. B. Collings, A. Forenza, and R. W. Heath Jr., "Multiplexing/beamforming switching for coded-MIMO in spatially-correlated channels based on closed-form BER approximations," *IEEE Trans. Veh. Technol.*, vol. 56, no. 5, part 1, pp. 2555–2567, Sept. 2007.

Antonio Forenza (S'04-M'06) received the M.S. degree in telecommunications engineering from Politecnico di Torino, Italy, and Eurecom Institute, Sophia Antipolis, France, in 2001, and the Ph.D. degree in electrical and computer engineering from The University of Texas at Austin, TX, in 2006.

In 2001 he interned as a Systems Engineer at Iospan Wireless, Inc., San Jose, CA, a startup company that developed the first commercial multiple-input multiple-output (MIMO) orthogonal frequency-division multiplexing (OFDM) communication system. His main research focus was on link adaptation and physical layer algorithm design. In the fall 2001 he joined ArrayComm, Inc., San Jose, CA, as a Systems Research Engineer. At ArrayComm, he was involved in the design and implementation of smart antenna systems for the 3G wireless platform. Over the summer 2004 and 2005 he interned as a Research Engineer at Samsung Advanced Institute of Technology, Suwon, Korea, and Freescale Semiconductor, Inc., Austin, TX, respectively, developing adaptive MIMO transmission and multiuser MIMO precoding techniques for 3GPP, IEEE 802.11n and IEEE 802.16e standards systems. Since June 2006, he has been working for Rearden, LLC, San Francisco, CA, as a Senior Systems Engineer.

Dr. Forenza authored the IEEE VTC'06 Best Student Paper Award. His research interests include MIMO antenna design, adaptive MIMO transmission techniques, precoding methods for MU-MIMO, smart antenna signal processing.

Robert W. Heath Jr. (S'96-M'01-SM'06) received the B.S. and M.S. degrees from the University of Virginia, Charlottesville, VA, in 1996 and 1997 respectively, and the Ph.D. from Stanford University, Stanford, CA, in 2002, all in electrical engineering.

From 1998 to 2001, he was a Senior Member of the Technical Staff then a Senior Consultant at Iospan Wireless Inc, San Jose, CA where he worked on the design and implementation of the physical and link layers of the first commercial MIMO-OFDM communication system. In 2003 he founded MIMO Wireless Inc, consulting company dedicated to the advancement of MIMO technology. Since January 2002, he has been with the Department of Electrical and Computer Engineering at The University of Texas at Austin where he is currently an Associate Professor and a member of the Wireless Networking and Communications Group. His research interests cover a broad range of MIMO communication including limited feedback techniques, antenna design, relaying, ad hoc networking, and scheduling algorithms as well as 60GHz communication techniques.

Dr. Heath has been an Editor for the IEEE TRANSACTIONS ON COMMUNICATION and an Associate Editor for the IEEE TRANSACTIONS ON VEHICULAR TECHNOLOGY. He is a member of the Signal Processing for Communications Technical Committee in the IEEE Signal Processing Society. He was a technical co-chair for the 2007 Fall Vehicular Technology Conference, general chair of the 2008 Communication Theory Workshop, and is a general co-chair and co-organizer of the 2009 Signal Processing for Wireless Communications Workshop. He is the recipient of the David and Doris Lybarger Endowed Faculty Fellowship in Engineering and is a registered Professional Engineer in Texas.